RELEASED DICLOFENAC SODIUM SALT FROM CHITOSAN EMBEDDING IN A HYDROGEL MATRIX. A THEORETICAL AND EXPERIMENTAL STUDY

Maricel AGOP[1, 2], Vlad GHIZDOVAT[3], Tudor PETRESCU[4], Iuliana OPREA[5], Maria-Alexandra PAUN [6], Vladimir-Alexandru PAUN[7], Viorel-Puiu PAUN[1,8], Simona VOLOVAT[9]

Two formulations embedding diclofenac sodium salt into a chitosan hydrogel matrix with different crosslinking degree were prepared by in situ hydrogelation. The formulations were investigated by polarized light microscopy and scanning electron microscopy, and the in vitro drug release was tested in a medium mimicking the physiological environment. The mechanism of the drug release has been assessed by a theoretical model which was developed and it was based on the multifractal theory of motion. The drug release mechanism are described through continuous and non-differentiable curves – multifractal curves.

Keywords: drug release, chitosan, diclofenac sodium salt, hydrogel matrix, multifractal model

1. Introduction

Drug delivery became an extremely important field of medicine, mainly targeting to suppress the secondary effects of the systemic administration of drugs, by prompting a prolonged, controlled release [1, 2]. Many attempts were done in this prolific domain, consisting in developing new approaches, formulations and technologies for safely transporting bioactive compounds in a controlled manner to assure a maximum therapeutic effect and minimum secondary consequences. Among formulations, those based on hydrogels are of particular interest, due to the

[1] Academy of Romanian Scientists, 54 Splaiul Independentei, sector 5, 050094 Bucharest, Romania
[2]Department of Physics, "Gh. Asachi" Technical University of Iasi, 700050 Iasi, Romania
[3]"Grigore T. Popa" University of Medicine and Pharmacy, Faculty of Medicine, Biophysics and Medical Physics Department, 16 University Str., Iasi - 700115, Romania
[4]Department of Structural Mechanics, "Gh. Asachi" Technical University of Iasi, 700050 Iasi, Romania
[5]Department of Mathematics, Colorado State University, USA
[6]School of Engineering, Swiss Federal Institute of Technology (EPFL), Route Cantonale, 1015 Lausanne, Switzerland
[7]Five Rescue Research Laboratory, 35 Quai d'Anjou, 75004, Paris, France
[8]Physics Department, Faculty of Applied Sciences, University Politehnica of Bucharest, 313 Splaiul Independentei, sector 6, RO-060042 Bucharest, Romania
[9] University of Medicine and Pharmacy Grigore T. Popa Iasi, Iasi, Romania

*Corresponding author, email: maria_paun2003@yahoo.com

similarity with *in vivo* environment: they embed large amounts of water, allow the diffusion of the active compounds and have similar rheological properties with tissues [3, 4]. All these reasons make hydrogels an excellent matrix for encapsulation of drugs and their prolonged release. Among hydrogels, those based on chitosan are especially important, because chitosan is a biopolymer which totally fulfills the requirements of the indwelling devices: it is biocompatible, biodegradable and its decomposition products are non-toxic for beings [5, 6]. The main concern related to the use of chitosan-based hydrogels for *in vivo* applications is the use of crosslinking agents, which usually have a toxicity degree [7]. Recent investigations related to the chitosan-based hydrogels revealed a new pathway for its crosslinking with natural originating monoaldehydes leading to hydrogels with no cytotoxic effect [8-12]. This new type of biomaterials demonstrated excellent ability to accommodate bioactive compounds such as drugs or fertilizers and to control their release by crosslinking density or by dilution of the system during *in situ* hydrogelation [13-16]. The analysis of the structure – *in vitro* release relationship of these systems suggested that a key role for the prolonged release effect is given by the strong intermolecular forces developed between the chitosan chains and the bioactive compound subjected to encapsulation. These forces start to develop during the hydrogelation process and are maintained in the hydrogel and xerogel state, respectively. The occurrence of such strong forces is favored by the slower crosslinking of chitosan with monoaldehydes compared with polyaldehydes. This suggests that the use of these hydrogels for encapsulation of drugs is beneficial not only due to the overcoming of the toxicity barrier but also because they promote the prolonged controlled release. The next step for the developing of these promising formulations to reach real life applications is a deeper understanding of the factors which control the prolonged release. To do this, we developed a mathematical model using the multifractal theory of motion based on the description of the drug release mechanism through multifractal curves.

2. Experimental setup

Materials

Chitosan of low molecular weight, salicylaldehyde, ethanol, glacial acetic acid, phosphate buffer (PBS) (pH=7.4), diclofenac sodium salt were bought from Aldrich and used as received.

Preparation of the formulations

A series of formulations were prepared by in situ encapsulation of diclofenac sodium salt during the hydrogelation of chitosan with salicylaldehyde, as described in the reference [14]. Shortly, the drug and monoaldehyde crosslinker were dissolved together in ethanol and then slowly dropped into a chitosan solution

under vigorous stirring. The amount of chitosan, salicylaldehyde and drug were chosen to give two formulations with different crosslinking density but constant amount of drug (Fig. 1).

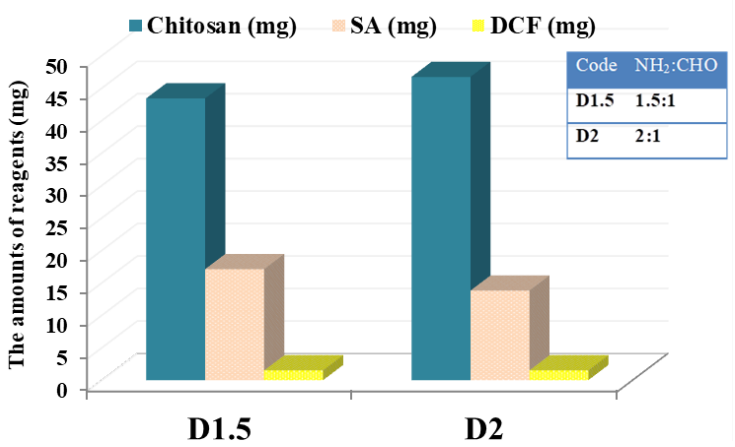

Fig. 1. Graphical representation of the components amounts of the drug delivery systems and their code

Equipment and methods

The as obtained formulations were lyophilized to give the corresponding xerogels, using a Labconco FreeZone Freeze Dry System equipment, for 24h at −54°C and 1.512mbar.

The morphology of the formulations was investigated by acquiring microimages of the xerogels on a Scanning Electron Microscope (SEM) EDAX – Quanta 200.

The xerogels were observed with a polarized light microscope Leica DM 2500 to evaluate the supramolecular ordering of the formulations and the physical state of the drug into the chitosan matrix.

The *in vitro* drug release was investigated during 10 days, mimicking a *in vivo* environment by using phosphate buffer solution (PBS) of pH 7.4 at body temperature of 37°C. Pellets of formulation xerogels were prepared using a hydraulic press ($2N/m^2$). The pellets were immersed into vials loaded with 10 mL PBS. At certain times, 2 mL aliquots were withdrawn and substituted with 2 mL neat PBS. The aliquots were subjected to UV-Vis spectrometry measurements to determine the drug released, by measuring the intensity of the specific band at 275 nm and fitting on a prior drawn calibration curve [14, 17]. The cumulative release of the *DCF* was estimated from the Lambert-Beer law. The UV-Vis spectra were recorded on an UV-visible spectrophotometer (Perkin Elmer, Lambda 10).

3. Results and Discussions

Two formulations were prepared by encapsulating diclofenac sodium salt into a chitosan based hydrogel, by varying the crosslinking density.

The analysis of the formulations by polarized light microscopy (POM) displayed strong birefringence as a continuous fine banded texture, characteristic for the layered supramolecular architectures (Figure 2. a, b) [18]. This is in agreement with the findings on the neat hydrogel [9], suggesting that the same hydrogelation pathway was preserved in the presence of the drug. No crystals of drug were found in the POM images, confirming that the most probably the drug was encapsulated into the hydrogel as submicrometric particles [19]. Comparing the images of the two formulations, it can be remarked a finer texture in the case of the hydrogel with higher crosslinking density (D1.5) in agreement with the tight structure with stronger intermolecular force imposed by the higher density of crosslinking nodes.

The layered architecture of the formulations was confirmed by the X-ray diffractograms too. As can be seen in the Figure 2c, the X-ray pattern consist from a two main broad reflections: one centered around 20 ^{o}, characteristic for the semicrystalline nature of chitosan, and another one around 6.5 ^{o}, characteristic for the layered ordering [9, 20, 21].

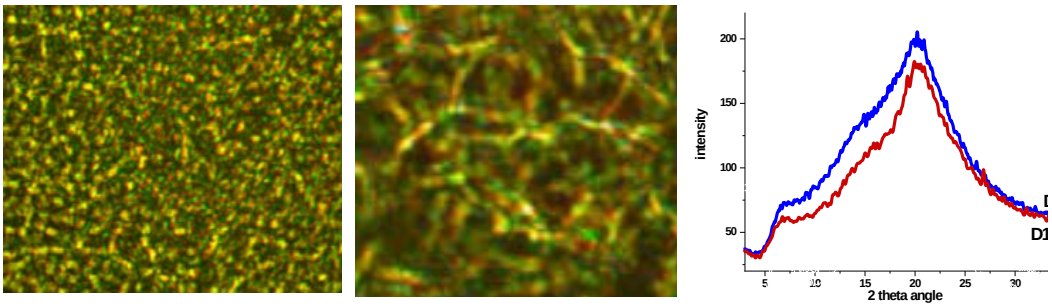

a) D1.5 **b) D2** **c)**

Fig. 2. a, b) POM images and c) X-ray diffractograms of the **D1.5** and **D2** formulations

The morphology of the hydrogels was studied by scanning electron microscopy. As can be seen in Figure 3, the higher crosslinking density reflected in smaller pores (D1.5) while a lower crosslinking density gave larger pores (D2) [22]. The lack of crystals in the POM images was confirmed by the SEM ones: geometrical shapes characteristic to drug crystals were observed neither in the pores nor in the pore walls. This definitely suggests that the drug was encapsulated into the bulk hydrogel at submicrometric level, under the detection limit of the SEM equipment.

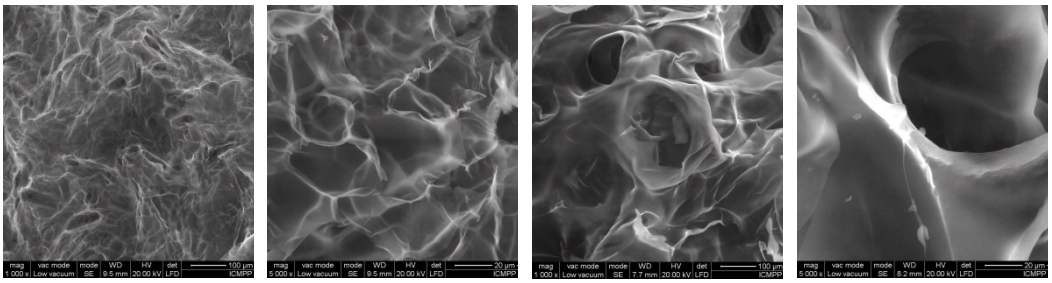

D1.5 **D1.5** **D2** **D2**

Fig. 3. SEM images of the **D1.5** and **D2** formulations

In vitro investigation given the release curves depicted in Figure 4. As can be seen both formulations showed a similar release trend, with some small differences. The hydrogel with higher crosslinking degree started to release the drug in a slower manner succeeding to release around 70 % in 10 days. This is simply explained by the tighter structure guided by the higher density of the crosslinking nodes which imposed a slower swelling of the matrix and made more difficult the diffusion of the drug molecules. On the other hand, the D2 released the drug faster, succeeding to release almost 80% of drug in the same period of time. This is a result of the lower crosslinking degree which allows a faster swelling of the hydrogel matrix and an easier diffusion of the drug molecules.

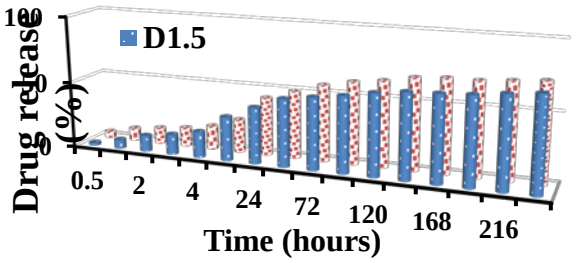

Fig. 4**.** Curves of the in vitro drug release of the diclofenac sodium salt form the chitosan based matrix

4. Theoretical model

Taking into account the complexity of the phenomena that take place in release processes (drug diffusion, erosion of polymer matrix, drug solubility etc.), it is admitted (evidently, as a work hypothesis) that this "complexity" can be "covered" by multifractality. In other words, the polymer – drug complex system release dynamics will be described through continuous and non – differential curves (multifractal curves, not monofractal curves, i.e. of a single fractal dimension D_F ,

as is the usual case in [23]). Then, the Multifractal Theory of Motion in its hydrodynamic form becomes functional through the equations [24, 25]:

$$\partial_t V_D^i + V^l \partial_l V_D^i = -\partial^i Q \tag{1}$$

$$\partial_t \rho + \partial^l \left(\rho V_D^l\right) = 0 \tag{2}$$

with

$$Q = 2\lambda^2 (dt)^{\left[\frac{2}{f(\alpha)}\right]-1} \frac{\partial_l \partial^l \sqrt{\rho}}{\sqrt{\rho}} \tag{3}$$

and

$$\partial_t = \frac{\partial}{\partial t}, \partial_l = \frac{\partial}{\partial X^l}, \ \partial_l \partial^l = \frac{\partial}{\partial X^l}\left(\frac{\partial}{\partial X^l}\right), \quad i, l = 1,2,3$$

In relations (1) – (4), t is the non-fractal time having the role of an affine parameter of the release curves, X^l is the multifractal spatial coordinate, V_D^i is the "multifractal fluid" velocity on differentiable scale resolution (the polymer – drug complex system is assimilated to a "multifractal fluid"; for details on the "behavior" of such a "physical object" – see [23-25]), ρ is the state density of the "multifractal fluid"[26-29], λ is the structural constant specific to the release process associated to the multifractal – non – multifractal transition, dt is the scale resolution and $f(\alpha)$ is the singularity spectrum of order α dependent on the fractal dimension D_F [30]. Operating with multifractal "manifolds" instead of monofractal ones (in the case of dynamic release systems) has some advantages:

i) areas of the polymer – drug complex system – of a certain fractal dimension – may be identified and can be characterized from a release dynamic viewpoint. From here, the number of zones of the polymer – drug complex system which have their fractal dimension in a certain interval of values may be identified;

ii) universality classes can be identified in the domain of dynamic release systems, even when the attractors have different aspects.

Equation (1) corresponds to the multifractal law of specific momentum conservation, equation (2) corresponds to the multifractal conservation law of state densities, while equation (3) corresponds to the multifractal specific potential as a measure of the multifractalization degree of the release curves.

The multifractal hydrodynamic system (1) – (3) admits, in a one-dimensional case, with clearly defined initial and boundary conditions, the solution (for details see [24, 25]):

$$V_D = \frac{V_0 \varepsilon^2 + \mu^2 x t}{\varepsilon^2 + \mu^2 t^2} \tag{4}$$

$$\rho = \frac{1}{\pi^{\frac{1}{2}}(\varepsilon^2 + \mu^2 t^2)^{\frac{1}{2}}} exp\left[-\frac{(x - V_0 t)^2}{\varepsilon^2 + \mu^2 t^2}\right] \tag{5}$$

where

$$\mu = \frac{2\lambda(dt)^{\left[\frac{2}{f(\alpha)}\right]-1}}{\varepsilon}, \tag{6}$$

V_0 is the initial velocity of the structural unit of the polymer – drug complex system, and ε is the "parameter" of the initial distribution of state densities:

$$\rho(x, t = 0) = \rho_0 exp\left[-\left(\frac{x}{\varepsilon}\right)^2\right], \qquad \rho_0 = const. \tag{7}$$

In normalized coordinates

$$\xi = \frac{x}{\varepsilon}, \qquad \eta = \frac{V_0 t}{\varepsilon}, \qquad V = \frac{V_D}{V_0}, \qquad \phi = \frac{\rho}{\rho_0}, \qquad \rho_0 = \frac{1}{\pi^{\frac{1}{2}}\varepsilon} \tag{8}$$

and normalized parameter

$$\sigma = \frac{2\lambda(dt)^{\left[\frac{2}{f(\alpha)}\right]-1}}{\varepsilon V_0}, \tag{9}$$

the solution of the multifractal hydrodynamic system in the normalized form becomes:

$$V = \frac{1 + \sigma^2 \xi\eta}{1 + \sigma^2 \eta^2} \tag{10}$$

$$\phi = \frac{1}{(1 + \sigma^2 \eta^2)^{\frac{1}{2}}} exp\left[-\frac{(\xi - \eta)^2}{1 + \sigma^2 \eta^2}\right] \tag{11}$$

Now, taking into account the significance of ρ (for details see [23-25]), the derivative of (11) with respect to η, so the expression:

$$\frac{\partial\phi}{\partial\eta} = \left[\frac{-\sigma^2\eta(1+\sigma^2\eta^2)+2(\xi-\eta)(1+\sigma^2\eta^2)+2(\xi-\eta)^2\sigma^2\eta}{(1+\sigma^2\eta^2)^{\frac{1}{2}}}\right] \times exp\left[-\frac{(\xi-\eta)^2}{1+\sigma^2\eta^2}\right], \tag{12}$$

by multiplying with the normalized mass of the polymer – drug complex system's structural unit, μ_0, allows the defining of the normalized released drug mass in the form:

$$P(\eta, \sigma, \mu) = \frac{M(\eta)}{M(\infty)} = -\mu_0 \frac{\partial\phi}{\partial\eta} \tag{13}$$

In (13), $M(\eta)$ corresponds to the drug mass released at the normalized moment η, while $M(\infty)$ corresponds to the drug mass released at the normalized moment $\eta(\infty)$.

Now, it is time to calibrate the theoretical model with respect to the previously presented experimental data. So, let us first admit that the release

dynamics of the polymer – drug complex system (assimilated to the "multifractal fluid" dynamics [31-34]) are "uniform".

Then, all the structural units of the polymer – drug complex system "support" constant velocity dynamics:

$$V \equiv 1 \Leftrightarrow V_D = V_0 \tag{14}$$

- see (10), for $\xi = \eta$, situation in which (13) with $\mu_0 \equiv 1$ chosen, takes the form:

$$\frac{M(\eta)}{M(\infty)} = \frac{\sigma^2 \eta}{(1+\sigma^2\eta^2)^{\frac{3}{2}}} \tag{15}$$

In Figure 5 we have represented the 3D (a) and the contour plot (b) representation of drug release quantity *M*, as defined through the multifractal theoretical model. We notice a steep increase followed by a saturation regime. This particular dependence follows well the empirical dependences seen in Figure 4. We notice that similar behavior can be found at various fractalization degree. A certain fractalization degree defined the dynamics of the drug release for one specific polymer-matrix-drug system. This means means that various configuration of drug-polymer systems will always be defined by functions similar to (15). The prediction given by our model can be easily seen that it reads true for diclofenac sodium salt release, as presented in Figure 4.

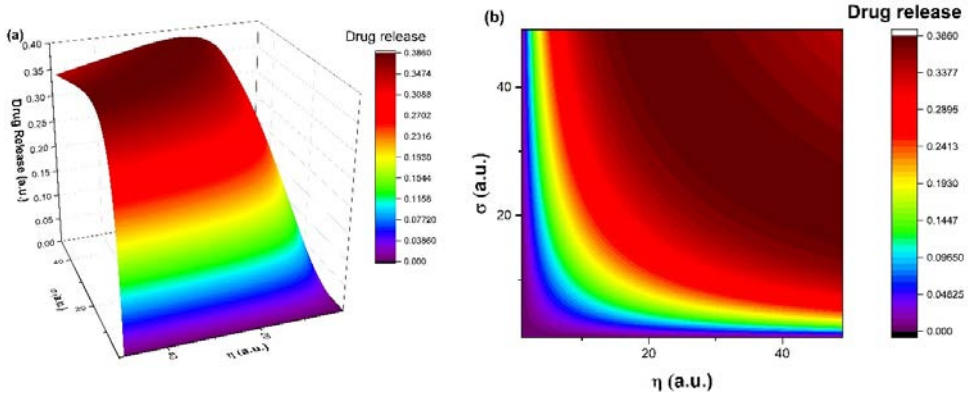

Fig. 5. (a) 3D theoretical dependencies related to the normalized time η
(b) fractalization σ function on the normalized time η

We present in Figures 5 a – b, the 3D and contour theoretical dependencies specified through (15) related to the normalized time η for various degrees of fractalization σ.

In Figure 6 we have represented the theoretical fit, based on our multifractal model, of the empirical data presented in Figure 4. The model follows well the experimental evolution, with a R-square of 99.8 for D2 data set and 98.7 for D1.5

data set. It results from Figure 6 that the theoretical model, through a convenient choice of the normalized parameters from (8), is validated based on experimental data presented in this work. We must note that, for $\sigma^2\eta^2 \ll 1$, (15) becomes:

$$\frac{M(\eta)}{M(\infty)} \to \sigma^2\eta, \tag{16}$$

situation in which the proposed model is reduced to the usual zero – order model, commonly used to describe the dissolution behaviour of modified – release pharmaceutical matrices and may also be used to describe the drug release from composite nanoparticles [35-37].

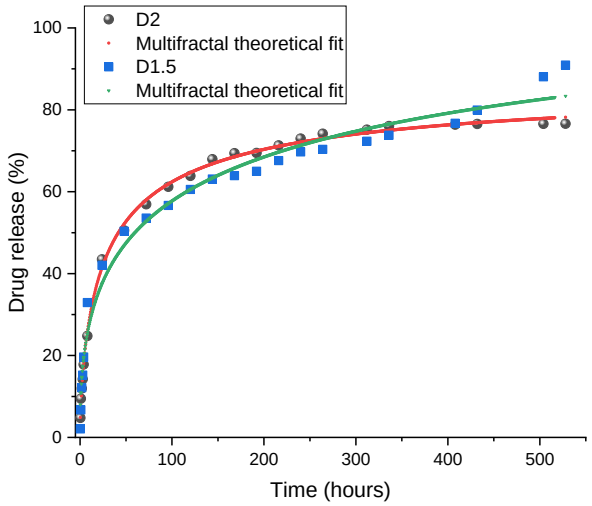

Fig. 6. Theoretical fit of the empirical data

The algorithms employed for the theoretical fit of the empirical data, based on the multifractal analysis, were first used in the articles [38-41].

5. Conclusions

Diclofenac sodium salt has been encapsulated into a chitosan based hydrogel by in sit hydrogelation with a monoaldehyde. The polarized light microscopy images indicated a hydrogelation pattern *via* a layered architecting. The scanning electron microscopy showed a microporous morphology with lower pores for a higher crosslinking density. The crosslinking density influenced the drug release by altering the diffusion process of the drug through the matrix. A mathematical model in the frame of the multifractal theory of motion, i.e. based on describing of the drug release mechanism through multifractal curves was developed. Finally, this model was validated by means of the experimental data.

REFERENCES

[1]. *C. Lia, J. Wangb, Y. Wangb, et al*., Recent progress in drug delivery, Acta Pharmaceutica Sinica B 9, 2019, pp. 1145-1162.

[2]. *Y. Wu, A. Rashidpour, M.P. Almajano, I. Metón*, Chitosan-Based Drug Delivery System: Applications in Fish Biotechnology, Polymers 12(5), 2020, 1177.

[3]. *X. Zhang, Y. Pan, S. Li, et al.,* Doubly crosslinked biodegradable hydrogels based on gellan gum and chitosan for drug delivery and wound dressing, International Journal of Biological Macromolecules, 164, 2020, pp. 2204-2214.

[4]. *M. Wang, Y. Shangguan and Q. Zheng*, Dynamics and Rheological Behavior of Chitosan-Grafted-Polyacrylamide in Aqueous Solution upon Heating, Polymers 12(4), 2020, 916.

[5]. *A. Ahsan, M. Asim Farooq, A. Parveen*, Thermosensitive Chitosan-Based Injectable Hydrogel as an Efficient Anticancer Drug Carrier, ACS Omega, 5, 32, 2020, pp. 20450–20460.

[6]. *N. Chaiwong, P. Leelapornpisid, K. Jantanasakulwong, et al*., Antioxidant and Moisturizing Properties of Carboxymethyl Chitosan with Different Molecular Weights, Polymers, 12(7) , 2020, 1445.

[7]. *R.O. Beauchamp, M.B. St Clair, T.R. Fennell, et al.,* A Critical Review of the Toxicology of Glutaraldehyde. Critical Reviews in Toxicology 22, 1992, pp. 143-174.

[8]. *L. Marin, D. Ailincai, S. Morariu, L. Tartau-Mititelu*, Development of biocompatible glycodynameric hydrogels joining two natural motifs by dynamic constitutional chemistry, Carbohydr. Polym. 170, 2017, pp. 60-71.

[9]. *M.M. Iftime, S. Morariu, L. Marin*, Salicyl- imine-chitosan hydrogels: Supramolecular architecturing as a crosslinking method toward multifunctional hydrogels, Carbohydr. Polym. 165, 2017, pp. 39-50.

[10]. *L. Marin, D. Ailincai, M. Mares, E. Paslaru, M. Cristea, V. Nica, B.C. Simionescu*, Iminochitosan biopolymeric films. Obtaining, self-assembling, surface and antimicrobial properties. Carbohydr. Polym. 117, 2015, pp. 762-770.

[11]. *M.M. Iftime, L. Marin*, Chiral betulin- imino-chitosan hydrogels by dynamic covalent sonochemistry, Ultrason. Sonochem. 45, 2018, pp. 238-247.

[12]. *A. Bejan, D. Ailincai, B.C. Simionescu, L. Marin*, Chitosan hydrogelation with a phenothiazine based aldehyde – toward highly luminescent biomaterials, Polym. Chem. 9, 2018, pp. 2359-2369.

[13]. *D. Ailincai, L. Mititelu-Tartau, L. Marin*, Drug delivery systems based on biocompatible imino-chitosan hydrogels for local anticancer therapy, Drug Deliv. 25, 2018, pp. 1080-1090.

[14]. *M.M. Iftime, L. Mititelu TartauL, L. Marin*, New formulations based on salicyl-imine-chitosan hydrogels for prolonged drug release, Int J Biol Macromol 160, 2020, pp. 398–408.

[15]. *A.M Craciun, L. Mititelu-Tartau, M. Pinteala, L. Marin*, Nitrosalicyl-imine-chitosan hydrogels based drug delivery systems for long term sustained release in local therapy, J. Colloid Interface Sci. 536, 2019, pp. 196-207.

[16]. *M.M. Iftime, G.L. Ailiesei, E. Ungureanu, et al.,* Designing chitosan based eco-friendly multifunctional soil conditioner systems with urea controlled release and water retention. Carbohydr Polym 223, 2019, 11504.

[17]. *Q. Yang, F. Yuan, L. Xu, et al*., An Update of Moisture Barrier Coating for Drug Delivery, Pharmaceutics, 11(9), 2019, 436.

[18]. *D. Iordache, S. Pusca, G. Toma*, et al., Analysis of compatibility with experimental data of Fractal descriptions of the fracture parameters, Conference: International Conference on Computational Science and its Applications (ICCSA 2006), Computational Science and Its Applications - ICCSA 2006, Pt 1_ Book Series: LECTURE NOTES IN COMPUTER SCIENCE, Vol. 3980, 2006, pp. 804-813.

[19]. *L. Marin, M.C. Popescu, A. Zabulica, H. Uji-I, E. Fron*, Chitosan as a matrix for biopolymer dispersed liquid crystal systems, Carbohydrate Polymers 95, 2013, pp. 16-24.
[20]. *S. Chen, M. Wu, C. Wang, S.Yan, P. Lu and S. Wang*, Developed Chitosan/Oregano Essential Oil Biocomposite Packaging Film Enhanced by Cellulose Nanofibril, Polymers 12(8), 2020, 1780.
[21]. *N. I. M. Fauzi, Y. W. Fen, N. A. S. Omar, S. Saleviter, W. M. E. M. M. Daniyal, H. S. Hashim, M. Nasrullah*, Nanostructured Chitosan/Maghemite Composites Thin Film for Potential Optical Detection of Mercury Ion by Surface Plasmon Resonance Investigation, Polymers 12(7), 2020, 1497.
[22]. *S. Xiong, L. Marin, L. Duan, X. Cheng*, Fluorescent chitosan hydrogel for highly and selectively sensing of p-nitrophenol and 2, 4, 6-trinitrophenol. Carbohydr Polym 225, 2019, 115253.
[23]. *M.V. Nichita, M.A. Paun, V.A. Paun, V.P. Paun*, Fractal Analysis of Brain Glial Cells. Fractal Dimension and Lacunarity, University Politehnica of Bucharest Scientific Bulletin-Series A-Applied Mathematics and Physics Vol. 81, no. 1, 2019, pp. 273-284.
[24]. *B. Lazar, A. Sterian, S. Pusca*, et al., Simulating delayed pulses in organic materials, Conference: International Conference on Computational Science and Its Applications (ICCSA 2006), Computational Science and Its Applications - ICCSA 2006, Pt 1 Book Series: LECTURE NOTES IN COMPUTER SCIENCE, Vol. 3980, 2006, pp. 779-784.
[25]. *M. Honciuc, V.P. Paun*, Liquid crystal-like behavior of some fatty acids mixtures. Revista de Chimie 54(1), 2003, pp. 74-76.
[26]. *S. Bungau, D.M. Tit, K. Fodor, et al*., Aspects Regarding the Pharmaceutical Waste Management in Romania. Sustainability 10, 2018, 2788.
[27]. *Paun, M.A., Cimpoesu, R., Cimpoesu, N., Agop, M., Baciu, C., Stratulat, S., Nejneru, C.*, Internal friction phenomena at polymeric and metallic shape memory materials, Materiale Plastice 47 (2), 2010, pp. 209-214.
[28]. *Agop M., Ioannou P., Nica P., Radu C., Alexandru A., Vizureanu P*., Fractal Characteristics of the Solidification Process, Materials Transactions 45 (3), 2004, pp. 972-975.
[29]. *M. Colotin, G.O. Pompilian, P. Nica, S. Gurlui, V. Paun, M. Agop*, Fractal Transport Phenomena through the scale relativity model, Acta Physica Polonica 116 (2), 2009.
[30]. *M.A. Paun, J.M. Sallese, M. Kayal*, A Circuit Model for CMOS Hall Cells Performance Evaluation including Temperature Effects, Advances in Condensed Matter Physics, Volume: 2013, Article Number: 968647.
[31]. *M. Agop, I. Mihaila, F. Nedeff, S.A. Irimiciuc*, Charged Particle Oscillations in Transient Plasmas Generated by Nanosecond Laser Ablation on Mg Target, Symmetry 12 (2) , 2020, 292.
[32]. *S.A. Irimiciuc, G. Bulai, S. Gurlui, M. Agop*, On the separation of particle flow during pulse laser deposition of heterogeneous materials-A multi-fractal approach, Powder technology 339, 2018, 273-280.
[33]. *S. Irimiciuc, F. Enescu, H. Bedelean, S. Gurlui, M. Agop*, Space-and time-resolved optical investigations on ns-laser produced plasmas on various geological samples Spectrochimica Acta Part B: Atomic Spectroscopy, 2020, 105904.
[34]. *S.A. Irimiciuc, B.C. Hodoroaba, G. Bulai, S. Gurlui, V. Craciun*, Multiple structure formation and molecule dynamics in transient plasmas generated by laser ablation of graphite, Spectrochimica Acta Part B: Atomic Spectroscopy 165, 2020, 105774.
[35]. *M. Agop, C. Murgulet*, El Naschie's ε (∞) space–time and scale relativity theory in the topological dimension D= 4, Chaos Solitons and Fractals 32(3), 2007, pp. 1231-1240.
[36]. *M. Agop, V. Paun, A. Harabagiu*, El Naschie's ε (∞) theory and effects of nanoparticle clustering on the heat transport in nanofluids, Chaos Solitons and Fractals 37(3), 2008, pp. 1269-1278.

[37]. *Kockisch, Sandra, et al*., Mucoadhesive, Triclosan-Loaded Polymer Microspheres for Application to the Oral Cavity: Preparation and Controlled Release Characteristics, European Journal of Pharmaceutics and Biopharmaceutics 59(1), 2005, pp. 207–216.

[38]. *M.V. Nichita, M.A. Paun, V.A. Paun, and V.P. Paun*, Image Clustering Algorithms to Identify Complicated Cerebral Diseases. Description and Comparison, IEEE ACCESS 8, 2020, pp. 88434-88442.

[39]. *D. Bordescu, M.A. Paun, V.A. Paun, and V.P. Paun*, Fractal analysis of Neuroimagistic. Lacunarity degree, a precious indicator in the detection of Alzheimer's disease, University POLITEHNICA of Bucharest Scientific Bulletin, Series A-Applied Mathematics and Physics, Vol. 80, no. 4, 2018, pp. 309-320.

[40]. *P. Postolache, Z. Borsos, V.A. Paun, and V.P. Paun*, New Way in Fractal Analysis of Pulmonary Medical Images, University Politehnica of Bucharest Scientific Bulletin-Series A-Applied Mathematics and Physics, vol. 80, no.1, 2018, pp. 313-322.

[41]. *V.P. Paun, F. Popentiu, V.A. Paun*, A 3D Simulation Model for Porous Polymer Network Formation, Materiale Plastice 46(2), 2009, pp.189-191 .